Journal of Magnetism and Magnetic Materials 474 (2019) 282–286

Contents lists available at ScienceDirect

Journal of Magnetism and Magnetic Materials

journal homepage: www.elsevier.com/locate/jmmm

Research articles

Superparamagnetic zinc ferrite: A correlation between high magnetizations and nanoparticle sizes as a function of reaction time via hydrothermal process

Caner Hasirci*, Oznur Karaagac, Hakan Köçkar

Physics Department, Science and Literature Faculty, Balikesir University, Cagis 10145, Balikesir, Turkey

ARTICLE INFO

Keywords:
Zinc ferrite nanoparticles
Hydrothermal method
Magnetic properties
Nanoparticle size
Superparamagnetism
Extrapolation

ABSTRACT

Superparamagnetic zinc ferrite nanoparticles with high magnetization were successfully synthesized by hydrothermal method at 110 ° C under different reaction times from 2 to 24 h. Elemental analysis of the nanoparticles determined by inductively coupled plasma atomic emission spectroscopy and energy dispersive X-ray spectrometer results proved that the samples are zinc ferrite. X-ray diffraction (XRD) and Fourier transmission infrared spectroscopy analysis displayed that zinc ferrite nanoparticles were single phase of cubic ferrite. The particles size, d_{XRD} of the nanoparticles calculated from XRD patterns increased as the reaction time increased. From the images of transmission electron microscopy (TEM), the particle sizes, d_{TEM} were also calculated and increased from 6.8 ± 2.5 to 10.6 ± 5.1 nm as the reaction time increased, which were consistent with the d_{XRD}. Magnetic measurements revealed that the magnetization curves of the synthesized nanoparticles show superparamagnetic behavior with zero coercivity and remanence. And, the magnetization values also increased to a maximum value of 30.8 emu/g (measured at 20 kOe) as the particle size increased to ~10 nm with the increase of reaction time. At this particle size limit, this is a considerable high value compared to the superparamagnetic zinc ferrite nanoparticles studies. Magnetization values were also extrapolated. It is seen that to a certain degree, the average particle sizes of the products and hence high maximum magnetization can be tuned by simply adjusting the parameter, reaction time by hydrothermal process.

1. Introduction

Recently, zinc ferrite nanoparticles have been extensively investigated by researchers due to interesting physical and chemical properties compared to their bulk counterparts. Zinc ferrite nanoparticles have also attracted attention because of their potential applications in the field of magnetic resonance imaging (MRI) [1–3], drug delivery [4,5], sensing applications [6] and magnetic hyperthermia [7,8]. Especially in MRI application, encapsulated mixed spinel zinc ferrite showed promising results for T2 relaxivity and sensitivity of detection which were higher than the values of clinically used MRI agent Feridex® [1]. In drug delivery study [4], higher anticancer and drug delivery effects were observed for chitosan coated zinc ferrite nanohybrid than polyethylene coated cobalt ferrite for curcumin. Zinc ferrite is one of the iron based cubic spinel structure, and indicates striking changes in its magnetic properties by reducing the grain size to the nano size range. It has normal spinel structure in which non-magnetic all Zn^{+2} ions occupy tetrahedral sites and all magnetic Fe^{+3} ions occupy octahedral sites [9]. The control of the particle size is very important because the properties of the nanocrystals strongly depend upon that. Properties of zinc ferrite nanoparticles are greatly sensitive to the synthesis method and its preparation conditions. Chinnasamy et al. [10] synthesized zinc ferrite nanoparticles by ball milling method from a mixture of α-Fe_2O_3 and ZnO. As the ball milling time increased, the magnetization of zinc ferrite nanoparticles at room temperature increased from ~2 to 11 emu/g and the particle size decreased from 90 to 11 nm. Gharagozlou et al. [11] prepared zinc ferrite nanoparticles by Pechini process. The saturation magnetization value increased from 0.72 to 7.21 emu/g when the average particles size rose from 18 to 62 nm. Roy et al. [12] prepared zinc ferrite nanoparticles of different particle size using co-precipitation method. The superparamagnetic-paramagnetic size limit of zinc ferrite nanoparticles was found to be 17 nm, and the saturation magnetization increased with the decrease of particle size from 17 to 6 nm. In the study of Yadav et al. [13], zinc ferrite nanoparticles were synthesized by honey-mediated sol-gel combustion method. With the increase of annealing temperature the

* Corresponding author.
E-mail addresses: cnrhasirci@gmail.com (C. Hasirci), karaagac@balikesir.edu.tr (O. Karaagac), hkockar@balikesir.edu.tr (H. Köçkar).

https://doi.org/10.1016/j.jmmm.2018.11.037
Received 21 June 2018; Received in revised form 1 November 2018; Accepted 5 November 2018
Available online 07 November 2018
0304-8853/

particle size increased and subsequently the saturation magnetization decreased from 12.81 to 1.39 emu/g when the particle size increased from 11 to 57 nm. Coercivity of the nanoparticles first decreased from 16 to 1 Oe with the increase of particle size from 11 to 55 nm and then increased to 26 Oe for the 57 nm zinc ferrite nanoparticles. Xue et al. [14] prepared zinc ferrite nanoparticles with single spinel-phase by a facile self-propagating combustion method varying the amount of glycine. The saturation magnetization was 10 emu/g when the particle size was 32 nm. Phuruangrat et al. [15] synthesized zinc ferrite nanoparticles by using microwave assisted hydrothermal method and obtained a saturation magnetization of 19.5 emu/g and coercivity of 9 Oe for 3.5 nm zinc ferrite nanoparticles. As seen, in recent years, many techniques have been developed to prepare magnetic zinc ferrite nanoparticles such as; ball milling, co-precipitation, sol-gel, thermal decomposition and hydrothermal method [16,17]. Among these techniques, hydrothermal method has attracted attention due to the superiorities such as; high purity, high crystallinity, good dispersion, low cost, controllable physical and chemical properties. And, the parameters of hydrothermal process can be controlled to obtain magnetic nanoparticles with desired properties. In this study, superparamagnetic zinc ferrite nanoparticles with high magnetization were synthesized by changing reaction time via the hydrothermal process at 110 °C. The samples displayed the zinc ferrite spinel structure. The remarkably high magnetization value of 30.8 emu/g was obtained which was compared to the superparamagnetic zinc ferrite nanoparticles studies as the particle size was 10.6 nm. From the results, it is revealed that the superparamagnetic zinc ferrite nanoparticles with high magnetizations can be obtained by varying the reaction time using hydrothermal process.

2. Experimental and methods

1 M $ZnCl_2$ (Merck, purity 98%) and 2 M $FeCl_3{\cdot}6H_2O$ (Sigma-Aldrich, purity 99%) were dissolved in 50 ml deionized water to obtain ion solution. All reagents used in the investigation were of analytical grade and used without further purification. The ion solutions were added to 50 ml 8 M NaOH (Merck, purity 98%) and stirred (1000 rpm) at 80 °C for an hour to obtain the precursor. 15 ml of the precursor was then transferred into a Teflon-lined stainless steel autoclave and maintained at 110 °C for 2, 4, 8, 12, 16 and 24 h, separately. After cooling to room temperature naturally, all products were washed several times with distilled water and finally dried at 60 °C for 3 h. The samples synthesized at 2, 4, 8, 12, 16 and 24 h were labeled as S2, S4, S8, S12, S16 and S24, respectively and given in Table 1.

Elemental composition of the nanoparticles was analyzed by using an energy dispersive X-ray spectrometer (EDX). The elemental analysis was also determined via inductively coupled plasma atomic emission spectroscopy (ICP-AES). The structure of the produced particles was determined by X-ray diffraction (XRD) using a Phillips PANalytical's X'Pert PRO X-ray diffractometer with Cu Kα radiation (λ = 0.15406 nm) in the 20–80° range. The average crystallite size was inferred from the peak broadening using Scherrer equation [18], considering Lorentz function. Fourier Transform Infrared spectra were measured using FTIR spectrometer Perkin Elmer-Spectrum Two. Spectrum was obtained between 370 and 4000 cm^{-1} by using KBr pellets. The particle size of the synthesized nanoparticles was investigated using TECNAI G2 F30 model transmission electron microscope (TEM) with working voltage of 200 kV. Mean particle size was calculated from TEM images by measuring the size of at least 100 particles via Image J software. The magnetic measurements were performed using a vibrating sample magnetometer (VSM) ADE EV9 Model at room temperature with the maximum applied magnetic field of 20 kOe with 1 Oe intervals. Maximum magnetization is the magnetization value measured at ± 20 kOe.

3. Results and discussion

Elemental analysis of the nanoparticles determined by ICP-AES showed that the molar ratios of Zn:Fe in the samples S2, S4, S8, S12, S16 and S24 were 0.35, 0.48, 0.53, 0.44, 0.45, and 0.45, respectively. In Table 1, results of elemental analysis are listed. The samples with the Zn:Fe ratios around 0.5 prove that they are zinc ferrite according to studies [19–21] but the ratio of sample S2 was lower. Further investigations by XRD (a slight shift to lower angles was observed in the 2θ values) and FTIR analysis displayed the sample S2 shows zinc ferrite structure. It may be interpreted that zinc ferrite structure may not be completely occurred due to the non-bonding of the zinc to oxygen in the spinel ferrite structure, and consequently the places of zinc ions may be empty for sample S2. The EDX analysis is also used to confirm the results by investigating the elemental composition of the selected samples S12 and S24. The Zn:Fe ratio was found to be 0.46 and 0.51 for S12 and S24, respectively.

The XRD patterns of zinc ferrite nanoparticles synthesized at 110 °C for 2, 4, 12, and 24 h are presented in Fig. 1. The diffraction peaks at 2θ values of 29.9°, 35.2°, 42.8°, 53.0°, 56.5°, 62.1° and 73.5° were indexed to the (2 2 0), (3 1 1), (4 0 0), (4 2 2), (5 1 1), (4 4 0) and (5 5 3) planes of zinc ferrite (JCPDS 002-4496), respectively. The diffraction peaks in the XRD pattern of the samples match well with the XRD data of the spinel structure of zinc ferrite. Furthermore, no other peaks of any impurities and secondary phases are observed. On the other hand, Yoo et al. [22] studied the effect of reaction time on the hydrothermal synthesis of zinc ferrite nanoparticles and found that a Fe_2O_3 phase exists when the reaction time increases to 12 h. They obtained pure zinc ferrite phase at low reaction times (5 h). In the pattern of sample S2, although a slight shift to lower angles was observed in the 2θ values, the same zinc ferrite structure was observed. The crystal size, d_{XRD} of the nanoparticles was calculated from the most intense peak (3 1 1) by using the Scherrer's Formula [18]:

$$d_{XRD} = \frac{0.9\lambda}{\beta cos\theta} \quad (1)$$

where d_{XRD} is particle size (nm), β is the broadening of the diffraction

Table 1
Synthesis conditions, elemental compositions, particle sizes and magnetic properties of zinc ferrite nanoparticles.

Sample	Reaction Time (h)	ICP Results			XRD Results		Particle Sizes	Magnetic Properties	
		Zn (%)	Fe (%)	Zn:Fe	a (nm)	d_{XRD} (nm)	d_{TEM} (nm)	*M_{MAX} (emu/g) (measured)	**M_{MAX} (emu/g) (extrapolated)
S2	2	26.1	74.9	0.35	0.83125	7.7	6.8 ± 2.5	25.5	31.4
S4	4	32.5	67.5	0.48	0.84610	8.7	8.7 ± 3.5	27.5	33.6
S8	8	34.7	65.3	0.53		–	–	29.1	34.8
S12	12	30.9	69.1	0.44	0.84573	10.1	9.3 ± 4.2	29.9	35.8
S16	16	31.0	69.0	0.45		–	–	30.7	36.3
S24	24	31.3	68.7	0.45	0.84525	10.0	10.6 ± 5.1	30.8	36.4

* M_{MAX}: Maximum magnetization value measured at applied magnetic field of ± 20 kOe.
** M_{MAX}: Maximum magnetization value extrapolated at magnetic field of ± 150 kOe.

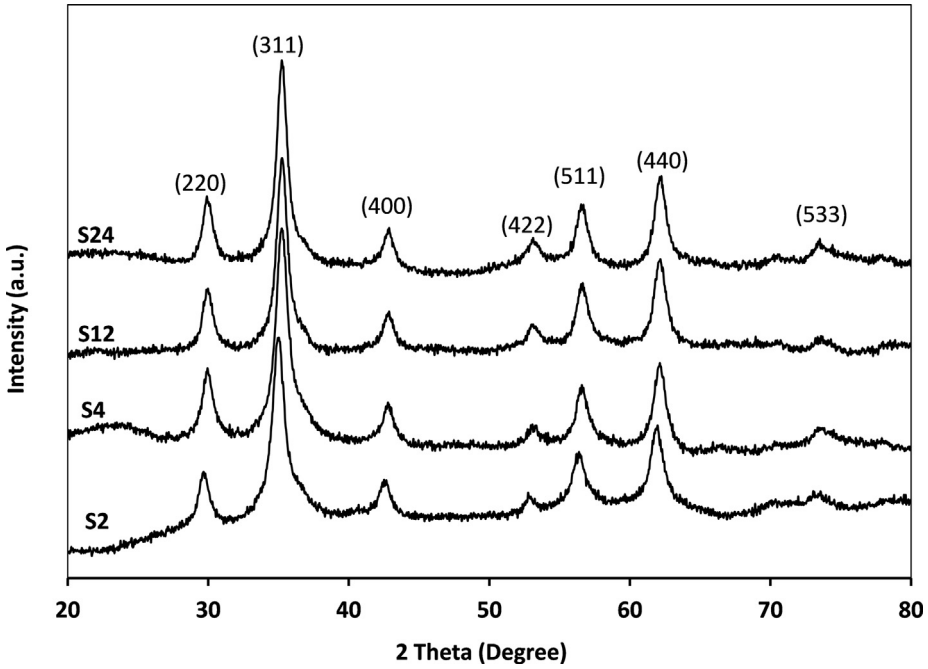

Fig. 1. XRD patterns of zinc ferrite nanoparticles synthesized at different reaction times; S2 (2 h), S4 (4 h), S12 (12 h) and S24 (24 h).

line measured at the half maximum intensity in radians, λ is the wave length of the used X-ray (1.5406 Å for C_u-Kα) and θ is Bragg angle of diffraction. The calculated d_{XRD} values are displayed in Table 1 as 7.7, 8.7, 10.1 and 10.0 nm for the samples S2, S4, S12 and S24, respectively. The d_{XRD} increases as the reaction time increases. The lattice constants, *a* were also calculated by using least squares technique and found to be 0.8313, 0.8461, 0.8457 and 0.8453 nm for the samples S2, S4, S12 and S24, respectively. The lattice constants of the samples are in agreement with the lattice constant of zinc ferrite (0.8350 nm). According to the ICP-AES and EDX results, Zn:Fe ratio for S2 sample was lower than other samples.

FTIR analysis was made for all samples and the spectra were given in the range of 370–1500 cm^{-1} in Fig. 2. In the FTIR spectrum of spinel ferrites, two main transmittance bands occur from atomic vibrations for the bonds between metal ions at octahedral or tetrahedral sites and oxygen ions. In Fig. 2, there are two transmittance bands observed at 558–552 cm^{-1} and 400–392 cm^{-1}. The band between 558 and 552 cm^{-1} corresponds to the intrinsic stretching vibration of Fe-O, whereas other band between 400 and 392 cm^{-1} corresponds to Zn-O ions at the octahedral site [23]. Also, Marzouk et al. [24] have found that the stretching vibration of the Fe-O bond is between 600 and 550 cm^{-1} at tetrahedral sites, and the stretching vibration of the Zn-O is between 450 and 385 cm^{-1} at octahedral sites. The transmittance peak at about 1068 cm^{-1} seen in Fig. 2 is related to Zn-Fe vibration according to [4]. Sawant et al. [4] have observed that stretching vibration of the Zn-Fe is between 1071 and 1115 cm^{-1}. The FTIR results confirm that the samples S2, S4, S8, S12, S16 and S24 have spinel structure of zinc ferrite, which is consistent with XRD results.

TEM images of the zinc ferrite nanoparticles synthesized at different reaction times are shown in Fig. 3(a–d). The calculated average particles sizes, d_{TEM} are presented in Table 1. The d_{TEM} are 6.8 ± 2.5, 8.7 ± 3.5, 9.3 ± 4.2, and 10.6 ± 5.1 nm for the samples S2, S4, S12 and S24, respectively. Also, the change in d_{TEM} values is consistent with the change of the d_{XRD} values. The size of nanoparticles increased with the increase of the reaction time from 2 h to 24 h at 110 °C. The number of small nanoparticles stays almost constant in all samples whereas the number of larger nanoparticles increases with the increase of reaction time. The observed changes may be explained by the incomplete consumption of the reactants after a short period. And, during the prolonged, longer time the reaction is likely to go to a more completion and thus larger particles are also obtained. High resolution TEM (HRTEM) image of a single zinc ferrite nanoparticle is shown in Fig. 3c. The interplane spacing was calculated as 0.251 nm from the image and the value corresponds to the (3 1 1) lattice plane of zinc ferrite confirming the XRD results.

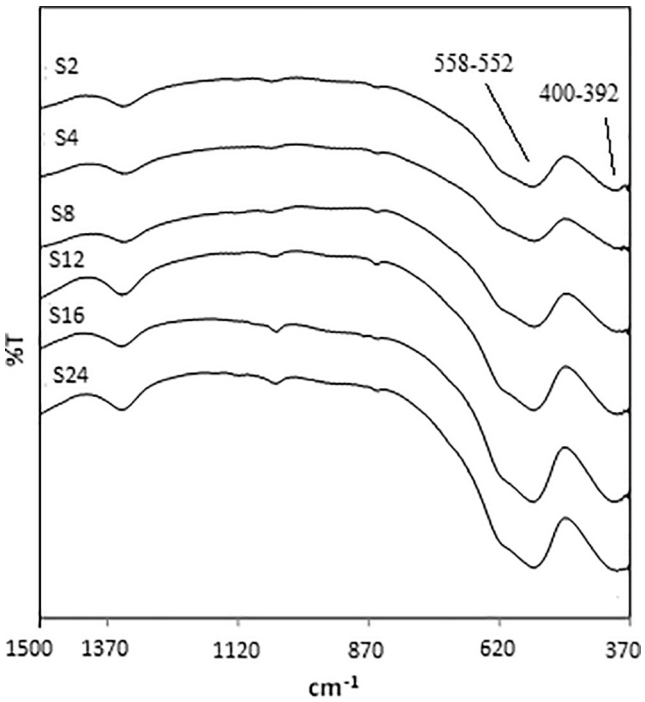

Fig. 2. FTIR spectra of zinc ferrite nanoparticles synthesized at different reaction times; S2 (2 h), S4 (4 h), S12 (12 h) and S24 (24 h).

The magnetization curves of samples S2, S4, S8, S12, S16 and S24 were measured at room temperature and presented in Fig. 4. It is evident that the prepared zinc ferrite nanoparticles have superparamagnetic behavior with zero coercivity and remanence, see Fig. 4. The maximum magnetizations (measured at the highest magnetic field

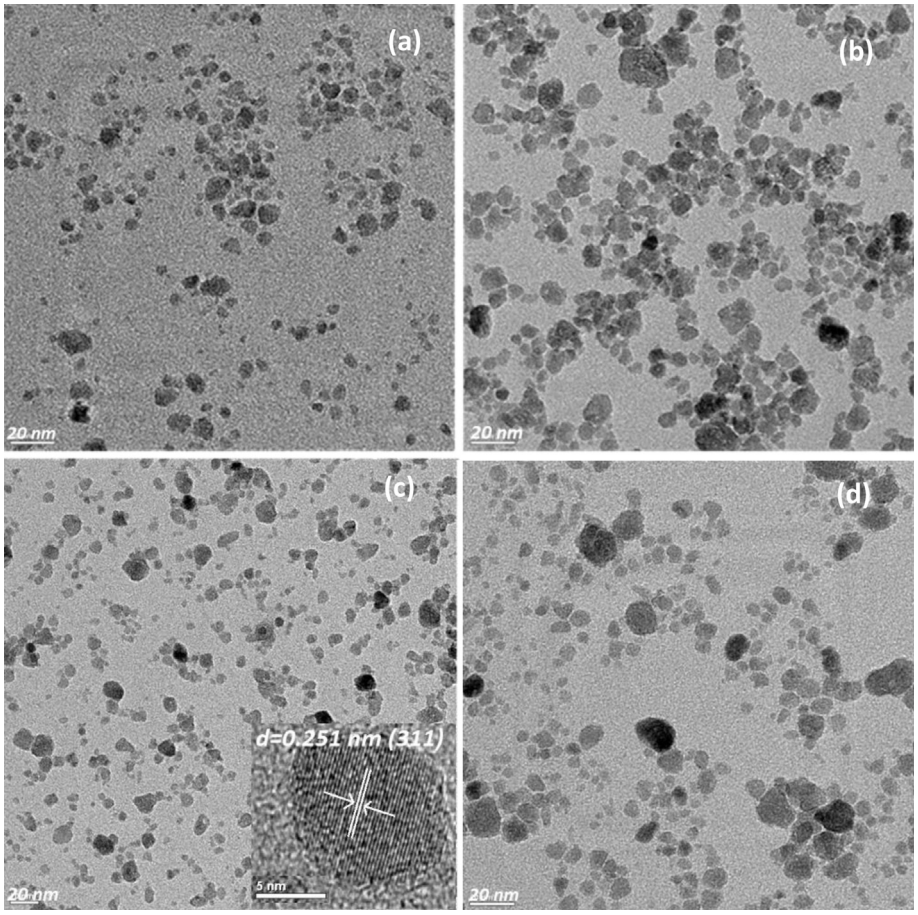

Fig. 3. TEM images for zinc ferrite nanoparticles synthesized with different reaction times; (a) 2 h (S2), (b) 4 h (S4), (c) 12 h (S12) with a HRTEM image of single zinc ferrite nanoparticle and (d) 24 h (S24).

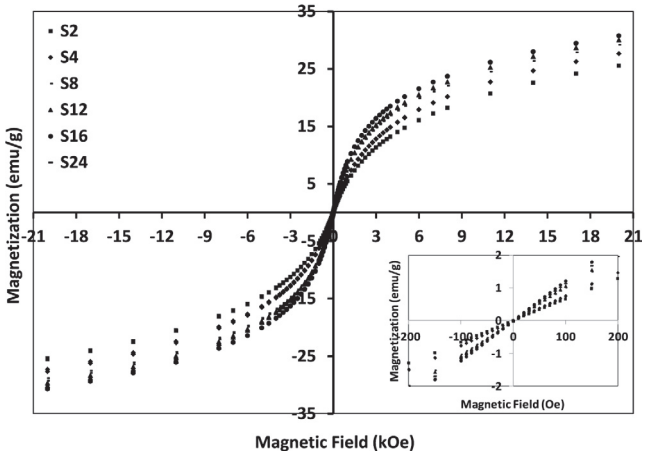

Fig. 4. Magnetization curves for zinc ferrite nanoparticles at room temperature with different reaction times; 2 h (S2), 4 h (S4), 8 h (S8), 12 h (S12), 16 h (S16), 24 h (S24) at 110 °C. Inset shows the magnetization curves with a field range of −200 to +200 Oe.

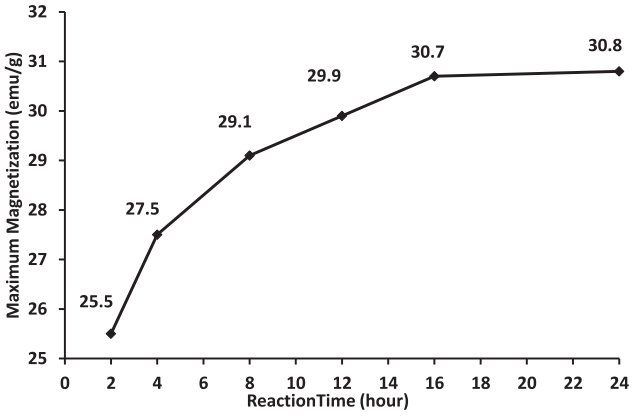

Fig. 5. Relationship of maximum magnetization and reaction time for zinc ferrite nanoparticles; S2 (2 h), S4 (4 h), S8 (8 h), S12 (12 h), S16 (16 h) and S24 (24 h).

of 20 kOe) of samples S2, S4, S8, S12, S16 and S24 are 25.5, 27.5, 29.1, 29.9, 30.7 and 30.8 emu/g, respectively, see Fig. 5. As seen from the figure, the magnetization values increase with the increase of particle size caused by the rise of reaction time. The magnetization values are considerably high compared to superparamagnetic zinc ferrite nanoparticles (with zero coercivity) synthesized by hydrothermal synthesis [20,22,26] and other techniques [12–14,25]. In the study [20], zinc ferrite nanoparticles synthesized by surfactant assisted hydrothermal process shows a paramagnetic-like behavior and maximum magnetization obtained at 15 kG is 6 emu/g. Yoo at al. [22] obtained pure superparamagnetic zinc ferrite nanoparticles (~60 nm) with a maximum magnetization of 8 emu/g (not saturated). Lestari et al. [26] synthesized zinc ferrite nanoparticles with hydrothermal and sol-gel methods. The nanoparticles obtained by hydrothermally are 32 nm and have a saturation magnetization of 34.4 emu/g with a small coercivity (2 Oe). As seen in the studies, particle size and hence the magnetic properties are dependent on the production conditions. In the same manner, in our study, it has been observed that the particle size of the zinc ferrite

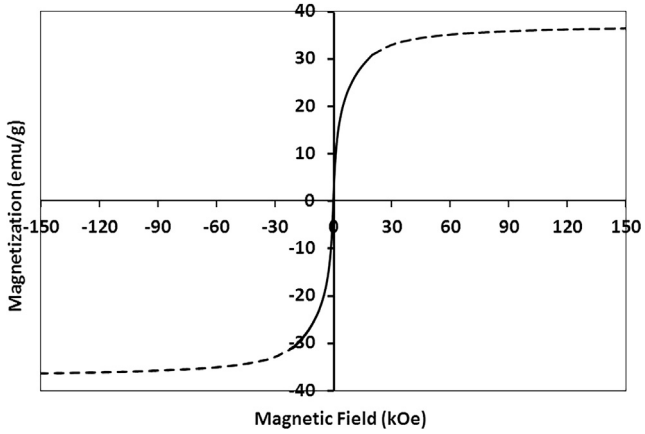

Fig. 6. Magnetization curve for sample S24 measured at ± 20 kOe (solid line) and extrapolated from ± 12.5 kOe to ± 150 kOe (dashed line).

nanoparticles and consequent magnetic properties depend on the reaction time of hydrothermal process. Besides, under study, 10.6 nm sized nanoparticles have 30.8 emu/g magnetization and zero coercivity, and the measured value at 20 kOe is the highest value among superparamagnetic zinc ferrite studies by now. Magnetization curves of samples showed that the magnetization does not saturate even for the high laboratory field (H = 20 kOe). In order to obtain the magnetization value at higher fields the magnetization data was extrapolated according to Eq. (2) [27] since the magnetization of zinc ferrite nanoparticles showed nearly linear dependence on magnetic field for the fields higher than 12.5 kOe.

$$M = M_o + \chi H \quad (2)$$

The estimated magnetization values of S2, S4, S8, S12, S16 and S24 samples at 150 kOe were listed in Table 1 as $^{**}M_{max}$ (extrapolated). The maximum magnetization of sample S24 reached up to 35.4 emu/g. The magnetization curves of sample S24 which were measured at ± 20 kOe and extrapolated at ± 150 kOe were given in Fig. 6 as an example. As expected, the higher magnetization values were estimated for superparamagnetic zinc ferrite nanoparticles at 150 kOe.

4. Conclusions

Superparamagnetic zinc ferrite nanoparticles with the highest magnetization were successfully prepared by hydrothermal method at 110 °C under its own conditions. The structural analysis revealed that the nanoparticles have high purity and single phase of zinc ferrite. The formation of spinel phase of zinc ferrite was investigated by the FTIR spectra confirming XRD results. The average particles size determined by TEM analysis was in the range of 6.8–10.6 nm. Magnetic measurements show that zinc ferrite samples exhibit superparamagnetic behavior at room temperature. And, the highest maximum magnetization of superparamagnetic zinc ferrite nanoparticles synthesized for 24 h at 110 °C was 30.8 emu/g. More importantly, magnetization values of the nanoparticles increased with the increase of particle sizes under the increase of the reaction time via hydrothermal process. The magnetization values were also extrapolated.

Acknowledgments

This work was supported by Balikesir University Research Grant No. BAP 2018/114. The authors would like to thank State Planning Organization, Turkey under Grant No 2005K120170 for VSM system, Balikesir University, Physics Department for FTIR analysis, Balikesir University, Science and Technology Application and Research Center for ICP-AES analysis, Bilkent University, Institute of Material Science and Nanotechnology, UNAM, Turkey for XRD, TEM and EDX measurements.

References

[1] C. Barcena, A.K. Sra, G.S. Chaubey, C. Khemtong, J.P. Liu, J. Gao, Zinc ferrite nanoparticles as MRI contrast agents, Chem. Commun. 19 (2008) 2224–2226.
[2] S.M. Hoque, C. Srivastav, N. Venkatesh, P.S. Anil Kumar, K. Chattopadhyay, Superparamagnetic behaviour and T_1, T_2 relaxivity of Zinc ferrite nanoparticles for magnetic resonance imaging, Philos. Mag. 93 (14) (2013) 1771–1783.
[3] S.M. Hoque, Md.S. Hossain, S. Choudhury, S. Akhter, F. Hyder, Synthesis and characterization of Zinc ferrite nanoparticles and its biomedical applications, Mater. Lett. 162 (2016) 60–63.
[4] V.J. Sawant, S.R. Bamane, R.V. Shejwal, S.B. Patil, Comparison of drug delivery potentials of surface functionalized cobalt and zinc ferrite nanohybrids for curcumin in to MCF-7 breast cancer cells, J. Magn. Magn. Mater. 417 (2016) 222–229.
[5] M. Sriramulu, D. Shukla, S. Sumathi, Aegle marmelos leaves extract mediated synthesis of zinc ferrite: antibacterial activity and drug delivery, Mater. Res. Express 5 (2018) 115404.
[6] R. Sahoo, S. Santra, C. Ray, A. Pal, Y. Negishi, S. Kumar Ray, T. Pal, Hierarchical growth of Zinc ferrite for sensing applications, New J. Chem. 40 (2016) 1861–1871.
[7] A. Hanini, L. Lartigue, J. Gavard, K. Kacem, C. Wilhelm, F. Gazeau, F. Chau, S. Ammar, Zinc substituted ferrite nanoparticles with $Zn_{0.9}Fe_{2.1}O_4$ formula used as heating agents for in vitro hyperthermia assay on glioma cells, J. Magn. Magn. Mater. 416 (2016) 315–320.
[8] T. Zargar, A. Kermanpur, Effects of hydrothermal process parameters on the physical, magnetic and thermal properties of $Zn_{0.3}Fe_{2.7}O_4$ nanoparticles for magnetic hyperthermia applications, Ceram. Int. 43 (2017) 5794–5804.
[9] R. Raeisi Shahraki, M. Ebrahimi, S.A. Seyyed Ebrahimi, S.M. Masoudpanah, Structural characterization and magnetic properties of superparamagnetic zinc ferrite nanoparticles synthesized by the coprecipitation method, J. Magn. Magn. Mater. 324 (2012) 3762–3765.
[10] C.N. Chinnasamy, A. Narayanasamy, N. Ponpandian, K. Chattopadhyay, H. Guérault, J-M. Greneche, Magnetic properties of nanostructured ferrimagnetic zinc ferrite, J. Phys.: Condens. Matter 12 (2000) 7795–7805.
[11] M. Gharagozlou, R. Bayati, Low temperature processing and magnetic properties of zinc ferrite nanoparticles, Superlatt. Microstruct. 78 (2015) 190–200.
[12] M.K. Roy, B. Haldarand, H.C. Verma, Characteristic length scales of nanosize zinc ferrite, Nanotechnology 17 (2006) 232–237.
[13] R.R. Singh Yadav, I. Kuřitka, J. Vilcakova, P. Urbánek, M. Machovsky, M. Masař, M. Holek, Structural, magnetic, optical, dielectric, electrical and modulus spectroscopic characteristics of Zinc ferrite spinel ferrite nanoparticles synthesized via honey-mediated sol-gel combustion method, J. Phys. Chem. Solids 110 (2017) 87–99.
[14] H. Xue, Z. Li, X. Wang, X. Fu, Facile synthesis of nanocrystalline zinc ferrite via a self-propagating combustion method, Mater. Lett. 61 (2007) 347–350.
[15] A. Phuruangrat, W. Maisang, T. Phonkhokkong, S. Thongtem, T. Thongtem, Superparamagnetic and ferromagnetic behaviour of ZnFe2O4 nanoparticles synthesized by microwave-assisted hydrothermal method, Russ. J. Phys. Chem. A 5 (2017) 951–956.
[16] A.S. Teja, P.-Y. Koh, Synthesis, properties, and applications of magnetic iron oxide nanoparticles, Prog. Cryst. Growth Charact. Mater. 55 (2009) 22–45.
[17] P. Srivastava, P.K. Sharma, A. Muheem, M.H. Warsi, Magnetic Nanoparticles: a review on stratagems of fabrication and its biomedical applications, Recent Pat. Drug Deliv. Formulation 11 (1) (2017) 1–13.
[18] B.D. Cullity, Elements of X-ray Diffraction, Addison-Wesley, USA, 1978.
[19] R. Rameshbabu, B. Neppolian, Surfactant assisted hydrothermal synthesis of superparamagnetic zinc ferrite nanoparticles as an efficient visible-light photocatalyst for the degradation of organic pollutant, J. Clust. Sci. 27 (2016) 1977–1987.
[20] R.K. Sharma, R. Ghose, Synthesis and characterization of nanocrystalline zinc ferrite spinel powders by homogeneous precipitation method, Ceram. Int. 41 (2015) 14684–14691.
[21] R. Rameshbabu, R. Ramesh, S. Kanagesan, A. Karthigeyan, S. Ponnusamy, Synthesis of superparamagnetic Zinc ferrite nanoparticle by surfactant assisted hydrothermal method, J. Mater. Sci: Mater. Electron 24 (2013) 4279–4283.
[22] P.S. Yoo, B.W. Lee, C. Liu, Effects of pH value, reaction time and filling pressure on the hydrothermal synthesis of ZnFe2O4 nanoparticles, IEEE Trans. Magn. 51 (1) (2015) 2003004.
[23] Y. Köseoğlu, A. Baykal, M.S. Toprak, F. Gözüak, A.C. Başaran, B. Aktas, Synthesis and characterization of Zinc ferrite magnetic nanoparticles via a PEG-assisted route, J. Alloy. Compd. 462 (2008) 209–213.
[24] A.A. Marzouk, A.M. Abu-Dief, A.A. Abdelhamid, Hydrothermal preparation and characterization of Zinc ferrite magnetic nanoparticles as an efficient heterogeneous catalyst for the synthesis of multi-substituted imidazoles and study of their anti-inflammatory activity, Appl. Organomet. Chem. 32 (2018) e3794.
[25] O.V. Yelenich, S.O. Solopan, T.V. Kolodiazhnyi, V.V. Dzyublyuk, A.I. Tovstolytkin, Magnetic properties and high heating efficiency of ZnFe2O4 nanoparticles, Mater. Chem. Phys. 146 (2014) 129–135.
[26] K.R. Lestari, P.S. Yoo, D.H. Kim, C. Liu, B.W. Lee, ZnFe2O4 nanoparticles prepared using the hydrothermal and sol-gel methods, J. Korean Phys. Soc. 66 (4) (2015) 651–655.
[27] C. Yao, Q. Zeng, G.F. Goya, T. Torres, J. Liu, H. Wu, M. Ge, Y. Zeng, Y. Wang, J.Z. Jiang, $ZnFe_2O_4$ nanocrystals: synthesis and magnetic properties, J. Phys. Chem. C 111 (2007) 12274–12278.